Resting GABA concentration predicts peak gamma frequency and fMRI amplitude in response to visual stimulation in humans

Suresh D. Muthukumaraswamy[a,1], Richard A.E. Edden[a,b,1], Derek K. Jones[a], Jennifer B. Swettenham[a], and Krish D. Singh[a,2]

[a]Cardiff University Brain Research Imaging Centre (CUBRIC), School of Psychology and [b]CUBRIC and Schools of Chemistry and Biosciences, Cardiff University, Cardiff CF10 3AT, United Kingdom

Edited by Leslie G. Ungerleider, National Institutes of Health, Bethesda, MD, and approved March 27, 2009 (received for review January 22, 2009)

Functional imaging of the human brain is an increasingly important technique for clinical and cognitive neuroscience research, with functional MRI (fMRI) of the blood oxygen level-dependent (BOLD) response and electroencephalography or magnetoencephalography (MEG) recordings of neural oscillations being 2 of the most popular approaches. However, the neural and physiological mechanisms that generate these responses are only partially understood and sources of interparticipant variability in these measures are rarely investigated. Here, we test the hypothesis that the properties of these neuroimaging metrics are related to individual levels of cortical inhibition by combining magnetic resonance spectroscopy to quantify resting GABA concentration in the visual cortex, MEG to measure stimulus-induced visual gamma oscillations and fMRI to measure the BOLD response to a simple visual grating stimulus. Our results demonstrate that across individuals gamma oscillation frequency is positively correlated with resting GABA concentration in visual cortex ($R = 0.68$; $P < 0.02$), BOLD magnitude is inversely correlated with resting GABA ($R = -0.64$; $P < 0.05$) and that gamma oscillation frequency is strongly inversely correlated with the magnitude of the BOLD response ($R = -0.88$; $P < 0.001$). Our results are therefore supportive of recent theories suggesting that these functional neuroimaging metrics are dependent on the excitation/inhibition balance in an individual's cortex and have important implications for the interpretation of functional imaging results, particularly when making between-group comparisons in clinical research.

functional magnetic resonance imaging | magnetic resonance spectroscopy | magnetoencephalography | oscillations

The high spatial resolution and noninvasive nature of blood oxygen level-dependent (BOLD) functional MRI (fMRI) (1) have led to it becoming one of the most popular tools for measuring brain function in human neuroscience. However, fMRI provides only an indirect measure of neural activity by measuring task-related changes in cerebral haemodynamics that are coupled by a complex and only partially understood mechanism to changes in underlying neural activity. Recent evidence suggests that oscillations in the gamma frequency range, loosely defined as approximately 30–100 Hz, are well correlated temporally, spatially, and functionally with haemodynamic changes in cortex, suggesting a close relationship with the BOLD response (2–6). There is also increasing evidence that the most plausible mechanism for the generation of gamma oscillations is a neuronal network containing a mixture of interconnected pyramidal cells and GABAergic inhibitory interneurons (7–10) with the balance of excitation-inhibition setting the peak gamma oscillation frequency of the network (11). Similarly, it has recently been argued that the magnitude of the BOLD response is also sensitive to this excitation-inhibition balance (12, 13).

In the current study, we tested the hypothesis that the local level of inhibition in an individual's brain contributes to the variability seen in both gamma oscillation frequency and BOLD response magnitude. As a measure of inhibition, the endogeneous resting concentration of GABA was quantified using edited magnetic resonance spectroscopy (MRS) (14) from a single voxel in the medial occipital pole. Magnetoencephalography MEG was used in the same participants to measure stimulus-induced sustained gamma oscillations in response to the presentation of a high-contrast, static, 3 cycle/degree grating patch. Similar low-level visual stimuli have previously been shown to be a strong inducer of gamma oscillations in the primary visual cortex of cats (15, 16) and humans (17–19). In subsequent recording sessions with the same participants, fMRI was used to measure the BOLD response in primary visual cortex to the identical visual stimulus used in the MEG.

Results

In all participants, resolved MRS peaks were observed for both Glx (combined glutamate/glutamine) and GABA metabolites (Fig. 1*B*) from a single voxel located in the medial occipital pole (Fig. 1*A*). By comparing the integral of the peak to an additional measurement of the unsuppressed water signal for the same volume, a measure of GABA concentration (quantified in institutional units) was calculated for each participant (see also supporting information (SI) Fig. S1).

Gamma frequency effects were localized in each individual using a nonlinear beamformer algorithm (20) and, in general, participants showed gamma oscillation responses that were confined to the right visual cortex, contralateral to the side of stimulation (Fig. 1*A* and Fig. S2). Placing a virtual electrode at the peak-source location and performing time-frequency analysis revealed a rich mixture of rapidly adapting onset responses and an induced gamma response that was sustained throughout stimulus presentation (Fig. 2*A*). There were clear differences in the peak frequency of this sustained gamma oscillation across our participants. This ranged between 40 and 66 Hz and, as with previous studies (21), is stable across repeat recording sessions (Fig. 2*B*). Gamma frequency and amplitude were not correlated ($R = 0.03$, $P = 0.9$).

When the metabolite concentrations were compared to the gamma oscillation frequency and magnitude, only the oscillation frequency was correlated with the level of GABA (frequency: $R = 0.68$, $P < 0.02$, Fig. 4 *Left*; amplitude: $R = -0.17$, $P = 0.6$).

Author contributions: S.D.M., R.A.E.E., J.B.S., and K.D.S. designed research; S.D.M. and R.A.E.E. performed research; S.D.M., R.A.E.E., and K.D.S. contributed new reagents/analytic tools; S.D.M., R.A.E.E., and D.K.J. analyzed data; and S.D.M., R.A.E.E., and K.D.S. wrote the paper.

The authors declare no conflict of interest.

This article is a PNAS Direct Submission.

[1]S.D.M. and R.A.E.E. contributed equally to this work.

[2]To whom correspondence should be addressed. E-mail: singhkd@cardiff.ac.uk.

This article contains supporting information online at www.pnas.org/cgi/content/full/0900728106/DCSupplemental.

www.pnas.org/cgi/doi/10.1073/pnas.0900728106

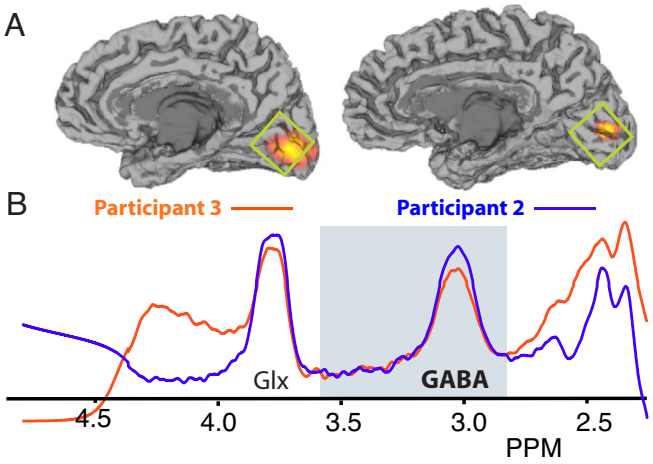

Fig. 1. Representative MEG and MRS data from 2 participants. (*A*) The location of significant ($P < 0.01$, corrected) induced gamma oscillations is shown on the individual MRIs of the 2 participants. Gamma power increases (orange/yellow) are clearly visible in the calcarine sulcus contralateral to the visual stimulus site. The green box shows the approximate position of the MRS acquisition voxel. (*B*) Edited MRS spectra for the 2 participants showing a well-resolved GABA peak. Fitted GABA MRS spectra for all participants are contained in Fig. S1.

We also investigated the dependency of gamma frequency and amplitude on age, Glx concentration in the same MRS voxel, and structural parameters within the medial occipital lobe, including gray matter thickness and total gray matter volume. No significant dependency was found on any of these parameters for either gamma magnitude or frequency (see Tables S1 and S2), although a trend toward significance was found for gamma amplitude and total lingual-cuneal gray matter volume ($R = 0.58$, $P = 0.06$).

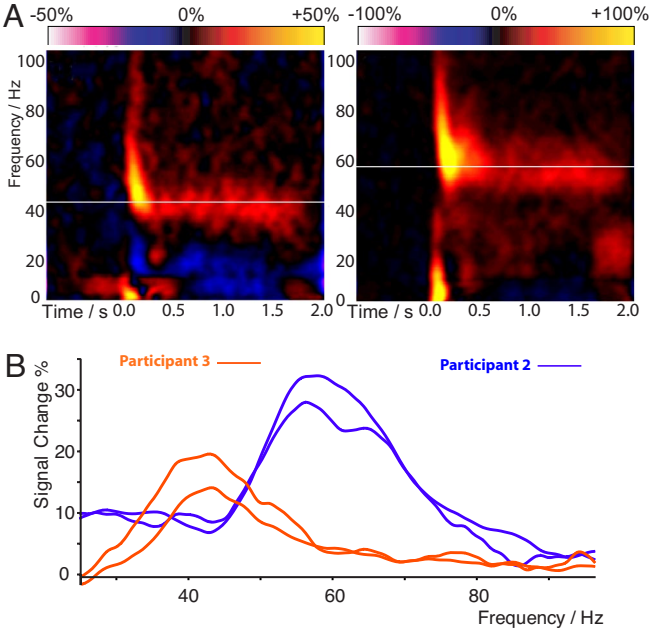

Fig. 2. (*A*) Time-frequency reconstructions for MEG activity at the maximal response position. Orange/yellow represents power increases and blue/purple power decreases from baseline. In each plot, the white line indicates the peak sustained gamma frequency that showed the greatest change in response to the stimulus. (*B*) The difference power spectrum for the same participants in Fig. 1 (orange and blue), averaged over the period from 0.5–2.0 s after stimulus onset. Intersubject differences are visible in both the frequency and amplitude of the gamma response. Note the stability of peak frequency across sessions, which were separated by at least 2 weeks for both participants. MEG source localization maps and time-frequency analyses for all participants are contained in Fig. S2.

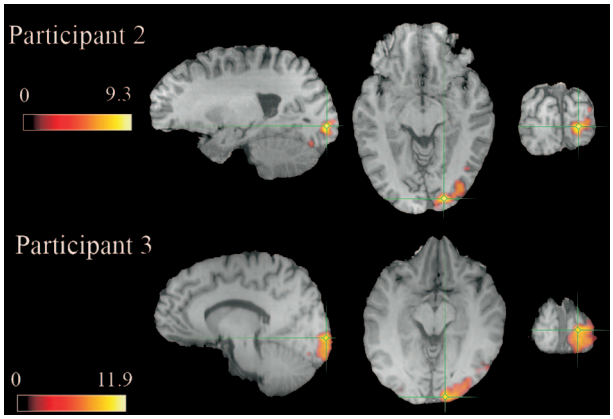

Fig. 3. Statistically thresholded ($P < 0.05$, corrected) BOLD activation for the 2 representative participants in Figs. 1 and 2 shown in sagittal, axial, and coronal views. Units are *z* scores. The green crosshair indicates the voxel with the maximum BOLD response. Similar maps for all participants can be found in Fig. S3.

As with the MEG recordings, we observed robust BOLD responses in the expected retinotopic area of primary visual cortex in all participants. Fig. 3 shows thresholded statistical probability maps of the BOLD response for the same representative participants in Figs. 1 and 2 (BOLD statistical probability maps for all participants can be found in Fig. S3). The magnitude of the BOLD response showed considerable variability across participants (range 0.9–2.5%). The magnitude of the BOLD response was negatively correlated with both GABA concentration ($R = -0.64$, $P < 0.05$, Fig. 4 center) and gamma oscillation frequency ($R = -0.88$, $P < 0.001$, Fig. 4 *Right*). BOLD amplitude did not correlate with gamma magnitude or other structural variables (see Tables S1 and S2).

Discussion

In this experiment, we found, across participants, that the endogenous resting concentration of GABA was positively correlated with the frequency of stimulus-induced gamma oscillations in medial occipital cortex. This result is consistent with a recent modeling study by Brunel and Wang (11) of a realistic cortical network in which interneurons and excitatory pyramidal cells are interconnected in reentrant loops. In this network, the dominant population response occurs in the gamma frequency range of 30–100 Hz and depends strongly on the ratio between excitatory and inhibitory connections and their time constants. Consistent with our current data, this mixed model predicts that as inhibition increases, the excitation/inhibition ratio will decrease and the dominant frequency will increase. One important feature of this model is that it predicts the emergence of gamma oscillations in coupled ensembles of inhibitory interneurons and pyramidal cells when the activity of individual neurons shows little evidence of firing in the gamma power band. This behavior has been found in monkey primary visual cortex (22) in which a gamma band peak is seen in the power spectrum of local-field potentials (LFPs) at high contrast but not in the firing of individual neurons, although other studies have also found that some cells in visual cortex show intrinsic gamma bursting or chattering (23). Evidence from hippocampal slice recordings shows that gamma oscillations are observed both in population activity and the firing profiles of individual inhibitory interneu-

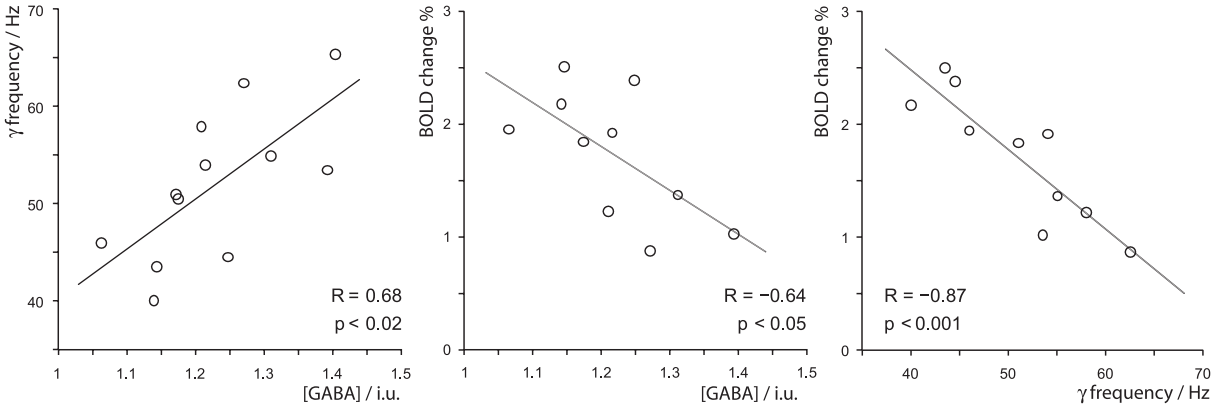

Fig. 4. Graphs, with best-fit linear regression lines, showing for each participant (*Left*) peak gamma oscillation frequency versus GABA concentration (*Center*) BOLD response magnitude versus GABA concentration and (*Right*) BOLD response magnitude versus peak gamma oscillation frequency.

rons (9, 24). In these intrinsically oscillating hippocampal cells, GABA appears to have the opposite effect to that predicted by the Brunel and Wang model (11) and our data, that is, as inhibitory drive is reduced by application of bicuculline, gamma oscillation frequency actually increases (9). Our data, in which gamma frequency increases with increasing GABA, is therefore more consistent with the ensemble properties of the Brunel and Wang model (11) rather than a model in which gamma oscillations arise from the firing properties of individual cells. In interpreting our results, it is important to remember that the bulk concentration of GABA present in the MRS voxel does not necessarily reflect the ability of GABA to locally modulate the excitation-inhibition balance within pyramidal-interneuron networks and hence modulate both the BOLD response and oscillation frequency. However, the fact that we do observe such a strong correlation suggests that MRS measures of bulk concentration do indeed provide a window into this network property. Ultimately, these issues can only be properly resolved by experiments examining how pharmacological manipulation of GABA affects the oscillatory dynamics of both single neurons and LFP ensemble activity in stimulus driven responses in visual or other sensory cortices. To our knowledge, unlike in the hippocampus, such experiments have not yet been performed.

In this study, no correlation was found between the Glx measure and any of the other parameters we studied. This is perhaps surprising, as glutamate should play an important role in the determination of the excitation/inhibition balance in cortex. However, Glx reflects a mix of both glutamate and glutamine and the ^{1}H 3-Tesla MRS sequences used here are unable to separate the contributions of the 2 molecules. Estimates in the literature vary, but the cortical concentration of glutamine may be as high as 45% of the concentration of glutamate (25). Our inability to demonstrate any correlations with Glx may therefore be a consequence of the mixed nature of this measure. More complex future spectroscopic investigations, perhaps at higher field strengths or using other nuclei (such as ^{13}C), may well reveal the importance of glutamate in studies such as ours. In our data, we did note a trend to significance between gamma amplitude and total lingual-cuneal gray matter volume. One possible explanation for this trend is that individuals with a larger volume of gray matter show increased spatial summation across a greater number of available neurons and/or cortical columns, leading to a larger gamma oscillation in the resultant macroscopic MEG signal.

In the present experiment, we used a relatively fast boxcar design (2 seconds "on" 10 seconds "off") to make the BOLD and MEG stimulation paradigms and data as comparable as possible. While this boxcar is relatively short for an fMRI experiment, previous modeling work and empirical data demonstrate that robust, stimulus-specific BOLD responses can be found in a visual cortex with this or similar timing schemes (19, 26, 27). A further issue with the use of short boxcar fMRI designs is a potential resonance of the boxcar frequency of 0.08 Hz with the 0.1 Hz oscillation caused by pulsatile motion in the vascular bed (28, 29). This raises the possibility that the variability in BOLD amplitude that we measure is linked to individual variability in this vasomotion signal, rather than being of neural origin. The current data cannot provide evidence either for or against this explanation. However, previous fMRI data has shown that the spatial distribution of activity from short boxcar designs is very similar to that from longer boxcar designs and that there is no evidence of a resonance "spike" in the amplitude profile (26). However, this possible vasomotion confound still is a theoretical possibility and is a specific example of the more general issue that intersubject variability in vascular perfusion and reactivity may play a key role in the relationships we describe here. Future studies using, for example, MRI perfusion techniques should provide important information to address these issues.

The current experiment has focused on stimulus-induced gamma oscillations and BOLD responses, with both measures calculated relative to baseline, and found a correlation of these measures with resting (baseline) GABA levels. The relatively poor signal-to-noise of gamma oscillations in our data precludes an analysis of resting gamma frequency and amplitude as we see no evidence of a gamma signal in the resting power spectrum of our data. In some participants, there are indications of task-related suppression of the baseline alpha and beta rhythm following visual stimulation, for example in Fig. 2. Source-localization of these changes show that the main effects of alpha/beta desynchronization are typically an extended network of sources in extrastriate and posterior parietal cortices (19, 30). The alpha and beta desynchronization seen in our calcarine source reconstructions may therefore represent bleed from the imperfect spatial filtering analysis (20) rather than a true focal suppression of these rhythms in primary visual cortex.

Both gamma oscillation peak frequency and GABA concentration were found to be negatively correlated with the BOLD response amplitude across participants, such that increased inhibition and gamma oscillation frequency are associated with a reduced BOLD response magnitude. This is consistent with a recent study in rat somatosensory cortex (31), which measured the BOLD response after i.v. administration of vigabatrin, a drug that inhibits the action of GABA transaminase (GABA-T), which normally acts to break down GABA. This blocking of GABA-T resulted in increased GABA levels as measured with MRS and a significantly reduced BOLD response. In humans, a

recent study combining GABA MRS and fMRI demonstrated that the negative BOLD response in the anterior cingulate region of the default mode network increased with increasing GABA across participants (32). Taken together, these data suggest that individuals with relatively high GABA concentrations in an area will exhibit relatively small positive BOLD responses and relatively large negative BOLD responses.

In principle, there at least 2 routes by which GABA concentration could alter BOLD response magnitude across participants. Firstly, there is a body of evidence that demonstrates that GABAergic interneurons can directly affect local circulation by release of several vasoactive neuromodulators (33, 34). Interneuron activity could therefore, in parallel, drive gamma frequency and the BOLD response. Alternatively, the GABAergic influence on BOLD may take place via the pyramidal cells and the metabolic demands associated with glutamate cycling (35) with increased GABA activity creating less glutamatergic activity. Under this interpretation, visual stimulation increases the total population activity; however, circuits with increased GABA may show more dampened evoked excitatory activity leading to a decreased BOLD response. It is also known that cortical networks with lower oscillatory frequencies are capable of sustaining larger networks due to decreased inhibition and it has been shown that the application of GABA antagonists increases horizontal cortical spread of excitation (36) and increases cerebral oxygen consumption (37). Further studies will be required to better elucidate these mechanisms and additional recording of physiological factors such as baseline perfusion should prove informative. A need also exists to test the generality of these results across the cortex, although recent data in human anterior cingulate (32) and rat somatosensory cortex (31) suggest the dependence of BOLD on GABA concentration may be a widespread phenomenon in the brain.

The results we present here have important implications for the interpretation of fMRI data, particularly those employing between-group comparisons (e.g., patients versus controls) that look for BOLD group differences within the brain in response to a particular experimental paradigm. Our data suggests that if such differences are found they could potentially be explained by group differences in either global or local GABA concentration/gamma network frequency regardless of the actual experimental paradigm used to stimulate the response. This could lead to a different interpretation of these experiments (one based more on anatomical circuit properties rather than task) than might have previously been made, as GABA concentration is rarely measured in fMRI protocols. In the future, the measurement of GABA concentration might be a useful addition to fMRI protocols and could be used as a covariate in the analysis of group fMRI data. This should be relatively practical for some studies as the data can be acquired in the same imaging session, although a strong prior hypothesis is needed to place the MRS voxel.

The possible sensitivity of MEG measures to GABA-mediated inhibition also suggests that the measurement of induced gamma-oscillation frequency in an individual may be useful within the context of pharmacological manipulations or clinical populations. For example, it has been shown that gamma oscillations across the cortex are modulated by a variety of drug preparations, including a morphine-induced decrease in inhibition (38). Although studies in humans looking at changes in stimulus-induced visual gamma oscillations and their relationship to GABAergic compounds have yet to be performed, the GABAergic agonist diazepam has been shown to increase rolandic beta amplitude and decrease the frequency of oscillation measured using MEG (39). In terms of pharmacological studies, MEG provides added opportunities over MRS in that it is a time-resolved technique that could assess changes in oscillation frequency over relatively short periods of time (tens of seconds or minutes) allowing, for example, characterization of dose-response curves for drugs that are thought to modulate cortical inhibition.

The correlations we have found between BOLD amplitude, gamma band frequency and resting GABA concentration may also be an important consideration in studies of diseases where GABA abnormalities are thought to play a role, such as epilepsy or schizophrenia (40). For example, it has been proposed that impairment of GABA-mediated inhibition in schizophrenia may lead to a reduction in synchronized network oscillations (41). In epilepsy, it has previously been shown that a moderate decrease in synaptic inhibition within neocortex slice preparations can lead to synchronous epileptiform discharges (27) and patients also show increased evoked gamma responses in the gamma frequency range (42). However, the importance and possible mechanisms by which GABAergic inhibition might be implicated in epilepsy are complex (43) and combined MEG, fMRI, and MRS studies such as the one we report here may help in clarifying these issues.

Methods

Participants and Stimuli. Twelve healthy right-handed male volunteers with normal or corrected-to-normal vision (mean age 34.8) participated in the experiment after giving informed consent; MEG, MRS, and fMRI data were collected on separate days.

For the MEG and fMRI experiment, identical stimuli consisting of vertical, stationary, maximum-contrast, 3 cycles per degree, square-wave gratings were presented on a mean luminance background. Gamma corrected stimuli were presented in the lower left visual field and subtended 4° both horizontally and vertically, with the upper right corner of the stimulus located 0.5° horizontally and vertically from a small red fixation point. Participants were instructed to maintain fixation for the entire experiment and, to maintain attention, were instructed to press a response key as fast as possible at the termination of each stimulation period. For the MEG experiment the duration of each stimulus was 1.5–2 s followed by 2 s of fixation cross only. Two hundred stimuli were presented in a session and participants responded to the first 100 stimuli with either the right or left hand and for the second 100 trials with the opposite hand. The entire session took 20 min. For the fMRI experiment the duration of each stimulus was 1.5–2 s followed by 10 s of fixation cross only, with 42 events presented in the session. In the MEG a Mitsubishi Diamond Pro 2070 monitor controlled by Presentation software was used to present all stimuli (1024 × 768 pixel resolution, 100 Hz refresh). For the fMRI experiment, stimuli were controlled by a Visage and presented via a Canon Xeed SX60 (1024 × 768 pixel resolution, 60 Hz refresh).

MEG Methods. Whole-head MEG recordings were made using a CTF 275-channel radial gradiometer system sampled at 1200 Hz (0–300 Hz band-pass). Twenty-nine reference channels were recorded for noise cancellation purposes and the primary sensors were analyzed as synthetic third-order gradiometers (44). Three of the 275 channels were turned off due to excessive noise.

Offline, each dataset was band-pass filtered using a fourth order bidirectional IIR Butterworth filter into 4 frequency bands 0–20 Hz, 20–40 Hz, 40–60 Hz, and 60–80 Hz based on our previous work (19) using evenly spaced frequency bands for balanced covariance estimation (45). The SAM (synthetic aperture magnetometry) beamformer algorithm (20) was used to create differential images of source power for 1.5 s of baseline (−1.5–0 s) compared to 1.5 s of visual stimulation (0–1.5 s). Details of the calculation of SAM pseudoT source image statistics are described elsewhere (20, 44). To achieve MRI/MEG coregistration, before the MEG acquisition, fiduciary markers were placed at fixed distances from anatomical landmarks identifiable in the participant's anatomical MRIs (tragus, eye center). Fiduciary locations were verified afterward using high-resolution digital photographs. For source localization, a multiple local-spheres (46) forward model was derived by fitting spheres to the brain surface extracted by FSL's Brain Extraction Tool (47). Estimates of source power were at 4 mm isotropic voxel resolution for each participant and frequency-band.

The peak locations of activity in primary visual cortex for each participant were located in these images and virtual electrodes were generated for these locations by SAM beamformer reconstructions obtained using covariance matrices band-pass filtered between 0 and 100 Hz (20). Time-frequency analyses of these virtual electrodes were conducted using the Hilbert transform from 1 to 100 Hz in 0.5 Hz steps and represented as a percentage change from the average baseline value for each frequency band. From these time-

frequency spectra, peak gamma band frequency and amplitudes, expressed as percentage change from baseline, were obtained. Individual SAM images were thresholded using permutation testing (48) (1000 permutations; $P < 0.01$ corrected).

Magnetic Resonance Methods. Magnetic resonance (MR) data were acquired on a 3T GE scanner with an 8-channel receive-only head rf coil. For each participant we obtained a 3D FSPGR scan with 1 mm isotropic voxel resolution for use with the MEG and fMRI analyses and for assessment of cortical thickness and volume.

GABA-edited MR spectra were acquired from a $3 \times 3 \times 3$ cm^3 volume positioned medially in the occipital lobe using the MEGA-PRESS method (14, 49). As shown in Fig. 1, the lower face of the voxel was aligned with the cerebellar tentorium and the voxel was positioned so as to avoid including the sagittal sinus and to ensure the volume remained inside the occipital lobe. The following experimental parameters were used: TE = 68 ms; TR = 1800 ms; 512 transients of 2 k data points were acquired in 15 min; a 20 ms Gaussian editing pulse was applied at 1.9 ppm in alternate scans. Phased-array coil data were combined (using the first point of the unsuppressed water free induction decay signal) and spectra were processed by locally written software. Three hertz exponential line broadening and a high-pass water filter were applied, and the MEGA-PRESS difference spectrum was produced. The edited GABA signal at 3 ppm and the unsuppressed PRESS water signal were integrated; a concentration measurement in institutional units was derived by accounting for the editing efficiency and the T1 and T2 relaxation times of water and GABA. The integral of the GABA peak was calculated automatically using a linear fit of the baseline and a Gaussian fit to the peak itself (50). Two 15 min measurements were made and the mean concentration measurement was calculated for each participant.

fMRI data were acquired using a gradient echo EPI sequence taking 30 axial slices at 3 mm isotropic voxel resolution centered over the visual cortex using a 64×64 matrix size, echo time of 35 ms, 90° flip angle, and T_R of 2 s. fMRI data were analyzed using the FSL software library using the following preprocessing; motion correction using MCFLIRT (51), nonbrain removal using BET (47); spatial smoothing using a Gaussian kernel of FWHM 5 mm; mean-based intensity normalization of all volumes by the same factor and high-pass temporal filtering (Gaussian-weighted least-squares straight line fitting $\sigma = 50$ s). The GLM was used to model a 2/10 s boxcar for each stimulus, after convolution with a standard haemodynamic response function to account for haemodynamic effects. For registration, data were initially registered to a whole-brain EPI scan and then to the FSPGR scan. The peak BOLD response in primary visual cortex in the amplitude images was converted into percentage signal change. Statistical thresholding was performed using Gaussian random field theory for the whole brain volume at a corrected significance of $P = 0.05$ (52).

Freesurfer (53) was used to obtain measures of cortical volume and cortical thickness in the occipital lobe. These were calculated by averaging the reconstructed mesh surface area and thickness measures for the lingual and cuneal gyri, which effectively provides average measures for the medial aspect of the occipital cortex. This region matches the approximate position of the spectroscopy voxel and includes the pericalcarine region in which the gamma sources were localized by MEG and the peak BOLD response in primary visual cortex.

ACKNOWLEDGMENTS. The authors acknowledge pulse programming advice from Gareth Barker and Dikoma Shungu. R.E. holds a Research Councils United Kingdom fellowship. This work was supported by the Schools of Psychology, Biosciences, and Chemistry at Cardiff University and the Wales Institute of Cognitive Neuroscience. CUBRIC was established with support from the United Kingdom Department of Trade and Industry, Cardiff University, and the Welsh Assembly government.

1. Ogawa S, Lee TM, Nayak AS, Glynn P (1990) Oxygenation-sensitive contrast in m-resonance image of rodent brain at high magnetic-fields. *Magn Reson Med* 14:68–78.
2. Logothetis NK, Pauls J, Augath M, Trinath T, Oeltermann A (2001) Neurophysiological investigation of the basis of the fMRI signal. *Nature* 412:150–157.
3. Niessing J, et al. (2005) Hemodynamic signals correlate tightly with synchronized gamma oscillations. *Science* 309:948–951.
4. Kayser C, Kim M, Ugurbil K, Kim DS, Konig P (2004) A comparison of hemodynamic and neural responses in cat visual cortex using complex stimuli. *Cereb Cortex* 14:881–891.
5. Lachaux JP, et al. (2007) Relationship between task-related gamma oscillations and BOLD signal: New insights from combined fMRI and intracranial EEG. *Hum Brain Mapp* 28:1368–1375.
6. Mukamel R, et al. (2007) Coupling between neuronal firing, field potentials, and fMRI in Human Auditory Cortex. *Science* 309:951–954.
7. Llinas RR, Grace AA, Yarom Y (1991) Invitro neurons in mammalian cortical layer 4 exhibit intrinsic oscillatory activity in the 10-Hz to 50-Hz frequency-range. *Proc Natl Acad Sci USA* 88:897–901.
8. Bartos M, Vida I, Jonas P (2007) Synaptic mechanisms of synchronized gamma oscillations in inhibitory interneuron networks. *Nat Rev Neurosci* 8:45–56.
9. Traub RD, Whittington MA, Colling SB, Buzsaki G, Jefferys JGR (1996) Analysis of gamma rhythms in the rat hippocampus in vitro and in vivo. *J Physiol* 493:471–484.
10. Wang XJ, Buzsaki G (1996) Gamma oscillation by synaptic inhibition in a hippocampal interneuronal network model. *J Neurosci* 16:6402–6413.
11. Brunel N, Wang XJ (2003) What determines the frequency of fast network oscillations with irregular neural discharges? I. Synaptic dynamics and excitation-inhibition balance. *J Neurophysiol* 90:415–430.
12. Logothetis NK (2008) What we can do and what we cannot do with fMRI. *Nature* 453:869–878.
13. Buzsaki G, Kaila K, Raichle M (2007) Inhibition and brain work. *Neuron* 56:771–783.
14. Mescher M, Merkle H, Kirsch J, Garwood M, Gruetter R (1998) Simultaneous in vivo spectral editing and water suppression. *NMR Biomed* 11:266–272.
15. Gray CM, Singer W (1989) Stimulus-Specific Neuronal Oscillations in Orientation Columns of Cat Visual-Cortex. *Proc Natl Acad Sci USA* 86:1698–1702.
16. Kayser C, Salazar RF, Konig P (2003) Responses to natural scenes in cat V1. *J Neurophysiol* 90:1910–1920.
17. Adjamian P, et al. (2004) Induced visual illusions and gamma oscillations in human primary visual cortex. *Eur J Neurosci* 20:587–592.
18. Hall SD, et al. (2005) The missing link: Analogous human and primate cortical gamma oscillations. *NeuroImage* 26:13–17.
19. Muthukumaraswamy SD, Singh KD (2008) Spatiotemporal frequency tuning of BOLD and gamma band MEG responses compared in primary visual cortex. *NeuroImage* 40:1552–1560.
20. Robinson SE, Vrba J (1999) Functional neuroimaging by synthetic aperture manetometry (SAM). *Recent Advances in Biomagnetism*, eds Yoshimoto T, Kotani M, Kuriki S, Karibe H, Nakasato N (Tohoku Univ Press, Sendai, Japan), pp 302–305.
21. Hoogenboom N, Schoffelen JM, Oostenveld R, Parkes LM, Fries P (2006) Localizing human visual gamma-band activity in frequency, time and space. *NeuroImage* 29:764–773.
22. Henrie JA, Shapley R (2005) LFP power spectra in V1 cortex: The graded effect of stimulus contrast. *J Neurophysiol* 94:479–490.
23. Gray CM, McCormick DA (1996) Chattering cells: Superficial pyramidal neurons contributing to the generation of synchronous oscillations in the visual cortex. *Science* 274:109–113.
24. Whittington MA, Traub RD, Jefferys JGR (1995) Synchronized oscillations in interneuron networks driven by metabotropic glutamate-receptor activation. *Nature* 373:612–615.
25. Jang DP, et al. (2005) Interindividual reproducibility of glutamate quantification using 1.5-T proton magnetic resonance spectroscopy. *Magn Reson Med* 53:708–712.
26. Bandettini PA, Cox RW (2000) Event-related fMRI contrast when using constant interstimulus interval: Theory and experiment. *Magn Reson Med* 43:540–548.
27. Muthukumaraswamy SD, Singh KD (2008) Functional decoupling of BOLD and gamma-band amplitudes in human primary visual cortex. *Hum Brain Mapp.*
28. Mayhew JEW, et al. (1996) Cerebral vasomotion: A 0.1-Hz oscillation in reflected light imaging of neural activity. *NeuroImage* 4:183–193.
29. Elwell CE, Springett R, Hillman E, Delpy DT (1999) Oscillations in cerebral haemodynamics—Implications for functional activation studies. *Oxygen Transport to Tissue* XXI, Advances in Experimental Medicine and Biology 471 (Kluwer Academic/Plenum, New York), pp 57–65.
30. Brookes MJ, et al. (2005) GLM-beamformer method demonstrates stationary field, alpha ERD and gamma ERS co-localisation with fMRI BOLD response in visual cortex. *NeuroImage* 26:302–308.
31. Chen ZG, Silva AC, Yang JH, Shen J (2005) Elevated endogenous GABA level correlates with decreased fMRI signals in the rat brain during acute inhibition of GABA transaminase. *J Neurosci Res* 79:383–391.
32. Northoff G, et al. (2007) GABA concentrations in the human anterior cingulate cortex predict negative BOLD responses in fMRI. *Nat Neurosci* 10:1515–1517.
33. Hamel E (2006) Perivascular nerves and the regulation of cerebrovascular tone. *J Appl Physiology* 100:1059–1064.
34. Vaucher E, Tong XK, Cholet N, Lantin S, Hamel E (2000) GABA neurons provide a rich input to microvessels but not nitric oxide neurons in the rat cerebral cortex: A means for direct regulation of local cerebral blood flow. *J Comp Neurol* 421:161–171.
35. Bonvento G, Sibson N, Pellerin L (2002) Does glutamate image your thoughts? *Trends Neurosci* 25:359–364.
36. Chagnacamitai Y, Connors BW (1989) Horizontal spread of synchronized activity in neocortex and its control by GABA-mediated inhibition. *J Neurophysiol* 61:747–758.
37. Weiss HR, Liu X, Chi OZ (2008) Cerebral O-2 consumption in young Eker rats, effects of GABA blockade: Implications for autism. *Int J Dev Neurosci* 26:517–521.
38. Whittington MA, Traub RD, Faulkner HJ, Jefferys JGR, Chettiar K (1998) Morphine disrupts long-range synchrony of gamma oscillations in hippocampal slices. *Proc Natl Acad Sci USA* 95:5807–5811.
39. Jensen O, et al. (2005) On the human sensorimotor-cortex beta rhythm: Sources and modeling. *NeuroImage* 26:347–355.
40. Lewis DA, Hashimoto T, Volk DW (2005) Cortical inhibitory neurons and schizophrenia. *Nat Rev Neurosci* 6:312–324.

41. Gonzalez-Burgos G, Lewis DA (2008) GABA neurons and the mechanisms of network oscillations: Implications for understanding cortical dysfunction in schizophrenia. *Schizophr Bull* 34:944–961.
42. Parra J, et al. (2003) Gamma-band phase clustering and photosensitivity: Is there an underlying mechanism common to photosensitive epilepsy and visual perception? *Brain* 126:1164–1172.
43. Bernard C, Cossart R, Hirsch JC, Esclapez M, Ben-Ari Y (2000) What is GABAergic inhibition? How is it modified in epilepsy? *Epilepsia* 41:S90–S95.
44. Vrba J, Robinson SE (2001) Signal processing in magnetoencephalography. *Methods (Amsterdam, Neth.)* 25:249–271.
45. Brookes MJ, et al. (2007) Optimising experimental design for meg beamformer imaging. *NeuroImage* 39(4):1788–1802.
46. Huang MX, Mosher JC, Leahy RM (1999) A sensor-weighted overlapping-sphere head model and exhaustive head model comparison for MEG. *Phys Med Biol* 44:423–440.
47. Smith SM (2002) Fast robust automated brain extraction. *Hum Brain Mapp* 17:143–155.
48. Cheyne D, et al. (2003) Neuromagnetic imaging of cortical oscillations accompanying tactile stimulation. *Brain Res* 17:599–611.
49. Edden RAE, Barker PB (2007) Spatial effects in the detection of gamma-aminobutyric acid: Improved sensitivity at high fields using inner volume saturation. *Magn Reson Med* 58:1276–1282.
50. Marshall I, et al. (2000) Choice of spectroscopic lineshape model affects metabolite peak areas and area ratios. *Magn Reson Med* 44:646–649.
51. Jenkinson M, Bannister P, Brady M, Smith S (2002) Improved optimization for the robust and accurate linear registration and motion correction of brain images. *NeuroImage* 17:825–841.
52. Worsley (2001) Statistical analysis of activation images. *Functional MRI: An Introduction to Methods*, eds Jezzard P, Matthews PM, Smith SM (Oxford Univ Press, Oxford).
53. Dale AM, Fischl B, Sereno MI (1999) Cortical surface-based analysis—I. Segmentation and surface reconstruction. *NeuroImage* 9:179–194.